Journal of Non-Newtonian Fluid Mechanics, 4 (1978) 111—136

FLOW SINGULARITIES, POLYMER CHAIN EXTENSION AND HYDRODYNAMIC INSTABILITIES *

M.R. MACKLEY

School of Engineering and Applied Sciences, University of Sussex, Falmer, Brighton, Sussex (Gt. Britain)

Summary

Flow singularities where the fluid velocity is zero are examined in terms of their relevance to polymer chain extension and flow instabilities. The singular flows are subdivided into two and three dimensional flows and flows that do and do not contain rotational components. Methods by which these various flows can be generated are reviewed.

Theoretical considerations necessary to achieve flow induced polymer chain extension are briefly reviewed and the major conclusions presented in a simple form. The consequences of these conditions are then discussed in relation to the ability and manner in which chain extension can occur in various flows.

The significance of degenerate and non degenerate two dimensional flows is examined in terms of flow stability and observed changes in the topology of flows; in particular the relevance of degenerate critical points where the principal strain rate equals the rotation rate is discussed in relation to the birth of eddies. Finally, the effect that localized polymer chain extension can have in modifying various singular flows is examined. When polymer is added to the flow a possible reduction in the persistent strain rate together with changes in the topology of flows are both considered.

1. Introduction

In comparison to the extensive experimental and theoretical studies carried out on singularities in solids, the close examination of singularities in

* Presented at the British Society of Rheology Conference on General Rheology and Stretching Flows, Edinburgh, September 7—9, 1977.

fluid flow has been virtually ignored. One class of singularity that is of interest in fluid flow is the stagnation point, line and sheet where the fluid velocity is zero; in steady flows these singularities will remain stationary in space with time. An object of this paper will be to draw particular attention to the existence and relevance of these singularities in certain flows and also show the overall importance of these singularities in terms of ultimate polymer chain extension and phenomena related to flow instabilities.

Over the past seven years several flow devices have been developed by the author and his associates at Bristol. Most of the flows studied were of high symmetry containing at least one stagnation point and many have been limited to a steady two dimensional flow pattern. These flows can be generated fairly easily in the laboratory and their interpretation is relatively unambiguous. By contrast many practical flows, including turbulence, involve complex time dependent three dimensional flows which are extremely difficult to interpret; it is hoped that an understanding of the simpler flows will aid our understanding in the more complex cases.

Definitions

It is convenient to start by defining certain quantities which have become important during the course of this study.

Velocity gradients. In general a velocity gradient in a fluid is defined by a tensor,

$$\dot{\epsilon}_{ij} = \frac{\partial V_i}{\partial x_j}, \tag{1}$$

where V is a velocity at a position r. We may split this tensor into two components,

$$S_{ij} = \tfrac{1}{2}(\dot{\epsilon}_{ij} + \dot{\epsilon}_{ij}), \tag{2}$$

$$\omega_{ij} = \tfrac{1}{2}(\dot{\epsilon}_{ij} - \dot{\epsilon}_{ji}), \tag{3}$$

such that

$$\dot{\epsilon}_{ij} = S_{ij} + \omega_{ij}, \tag{4}$$

The first symmetric part, S_{ij}, represents a deforming strain rate and the latter antisymmetrical part, ω_{ij}, a rotation rate.

For two dimensional flows, the strain rate tensor has the form

$$S_{ij} = \begin{bmatrix} \dot{\epsilon}_{11} & \tfrac{1}{2}(\dot{\epsilon}_{12} + \dot{\epsilon}_{21}) \\ \tfrac{1}{2}(\dot{\epsilon}_{12} + \dot{\epsilon}_{21}) & \dot{\epsilon}_{22} \end{bmatrix}, \tag{5}$$

where the magnitude of the principal strain rate S for incompressible flows is given by

$$S = \sqrt{(-\det S_{ij})} \tag{6}$$

and the magnitude of the rotation rate ω is given by

$$\omega = \tfrac{1}{2}|\operatorname{curl} V|. \tag{7}$$

The magnitude of the rate of stretching of a non rotating fluid line defined as σ and named the persistent strain rate [1] is given by

$$\sigma = \sqrt{S^2 - \omega^2} \tag{8}$$

2. Singular flows

2.1 Singular flows containing little or no rotation

Flows that are free from rotation will have $\omega_{ij} = 0$. These flows in many respects represent the simplest possible class of flows, however with the notable exception of the work by Trouton [2] and G.I. Taylor [3], they received little early experimental attention. The rotation free two dimensional pure shearing flow has a velocity gradient tensor given by,

$$\dot{\epsilon}_{ij} = \begin{bmatrix} S & 0 & 0 \\ 0 & -S & 0 \\ 0 & 0 & 0 \end{bmatrix} \tag{9}$$

Assuming incompressibility, the streamlines of this two dimensional flow may be given simply by the stream potential ϕ of the flow where ϕ is given by

$$(V_x, V_y, V_z) = \left(\frac{\partial \phi}{\partial y}, \frac{-\partial \phi}{\partial x}, 0\right) \tag{10}$$

Streamlines are represented by lines of constant ϕ. Pure shearing flow, shown schematically in Fig. 1, has a stream function given by

$$\phi = Sxy \tag{11}$$

The singularity of the flow where the velocity is zero occurs at the origin and exists as a line $(0, 0, z)$. For any given plane the singularity is defined as a hyperbolic critical point.

Pure shearing flow can be achieved experimentally in a number of ways. Low velocity gradients (0—$\sim 10^2\ s^{-1}$) can be achieved using a four roll mill apparatus initially pioneered by G.I. Taylor [3] and later used by amongst others Giesekus [4] and Crowley et al. [5]. The apparatus consists of four symmetrically positioned rollers. When the rollers are rotated at equal speed and with a rotation sense indicated in Fig. 2 a good approximation to uniform pure shearing flow is obtained in the central region of the flow near the critical point; however the hyperbolic nature of the pure shearing streamlines is incompatible with the circular boundary of the rollers and therefore the flow cannot be entirely that of pure shearing right up to the edges of the rollers. The four roll mill apparatus can easily be used by immersing the

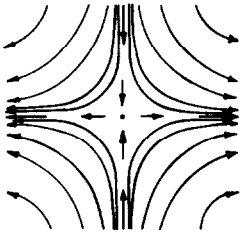

Fig. 1. Schematic diagram of streamlines for pure shearing flow.

rollers in a tank of fluid. Streamlines of the flow can be obtained by either viewing slight concentration differences in the flow using transmitted light, or by introducing small scattering particles such as Hostalen GUR polyethylene powder into the flow and viewing the optical scattering from a planar incident beam of light.

One of the problems with the four roll mill is that in general typical dimensions of the apparatus are large and of the order 1 cm thus turbulence can readily set in, particularly outside the central region of the rollers; this can restrict the maximum velocity gradient that can be achieved. To obtain high velocity gradients in pure shearing flow it would appear that a double

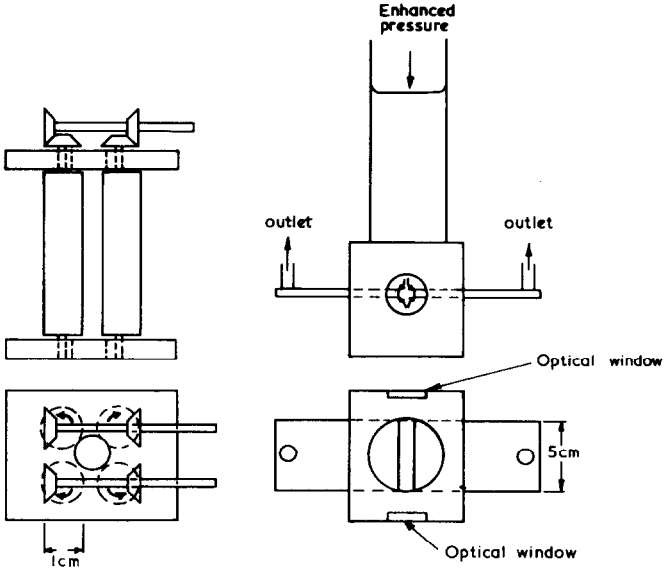

Fig. 2. Schematic diagram of four roll mill apparatus.

Fig. 3. Schematic diagram of double slit apparatus.

slit system is more satisfactory. The elements of such an apparatus are shown in Fig. 3. Using glycerol and polyethylene oxide solutions it was found that this apparatus could produce velocity gradients of up to 10^4 s^{-1} with the potential of higher velocity gradients being possible. Fluid is forced into the opposed slits by applying an enhanced pressure to the main cylinder. It was observed that the flow between the slits was close to that of uniform pure shearing flow and the ends or edges of the slits did not appear to interfere noticeably with the flow pattern. To a first approximation the magnitude of the velocity gradient can be given by $S = V/\delta$, where V is the centre line entry velocity into the slits and 2δ the separation of the slits; this approximation is valid for $\delta \leqslant \sim 2l$ where l is the internal diameter of the slits. When $\delta \geqslant \sim 2l$ the velocity gradient between the slits can no longer be considered uniform.

It is quite easy to devise other flows that will have regions containing singular pure shearing flows. A good example is the flow generated by two counter rotating rollers; this flow has two hyperbolic critical points shown schematically in Fig. 4. The asymptotic streamlines at the critical points intersect at right angles which indicate that the flow is that of pure shearing flow at this point. As indicated by the work of Jeffrey [6], in an ideal fluid the position of the critical points is controlled solely by the separation of the rollers, with the critical points moving outward with increasing roller separation. Another experimental arrangement of static cylinders in a steady translational flow, shown schematically in Fig. 5, is capable of generating an array of critical points. It has been indicated by Werlé [7] that at sufficient Reynolds number the vortices shed from each cylinder produce a symmetric flow pattern with a hyperbolic cricial point immediately downstream from each cylinder.

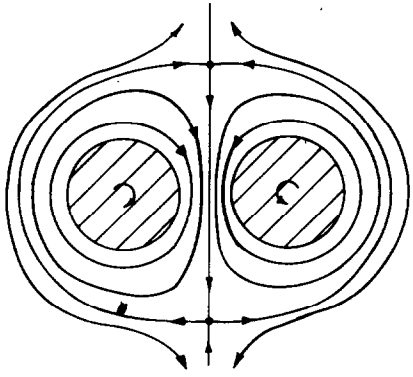

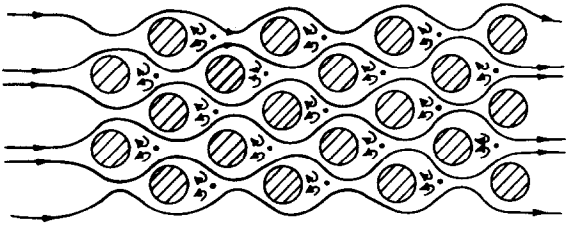

Fig. 4. Schematic diagram of flow between counter rotating rollers.

Fig. 5. Diagram of flow past a symmetric array of cylinders showing hyperbolic critical points downstream from each cylinder.

Three dimensional rotation free flows

One of the first flows to be studied at Bristol was the three dimensional flow produced by impinging jets [8,9]. This flow was of primary interest because it could produce essentially rotation free extensional flows of high velocity gradient. The system consists of two jets immersed in a "sea" of fluid. By forcing fluid out of the jets an axial compression flow would be produced in the region of jet impingement given by a velocity gradient tensor,

$$\dot{\epsilon}_{ij} = \begin{bmatrix} -S & 0 & 0 \\ 0 & \frac{1}{2}S & 0 \\ 0 & 0 & \frac{1}{2}S \end{bmatrix} \tag{12}$$

By reversing the flow and sucking fluid into the jets an axial extensional flow was achieved given by,

$$\dot{\epsilon}_{ij} = \begin{bmatrix} S & 0 & 0 \\ 0 & -\frac{1}{2}S & 0 \\ 0 & 0 & -\frac{1}{2}S \end{bmatrix} \tag{13}$$

For both axial compression and extension the singularity of the flow is a stagnation point which, using the classification of Poincaré (see for example ref. [10]), would be called a col singular point. The experimental realization of the flow is shown in Fig. 6. It was found that pure axial compression could only be achieved in a rather limited region of the flow close to the critical point [9]. The situation for axial extension was less stringent and providing the jet separation was less than about three jet diameters a good approximation to uniform axial extensional flow was achieved in the whole region between the jets.

2.2. Singular flows containing rotational components

At present both the experimental realization and theoretical considerations have concentrated on two dimensional rather than three dimensional

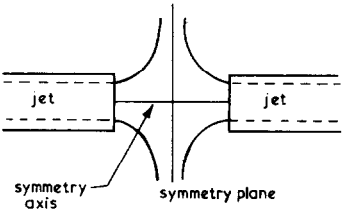

Fig. 6. Schematic diagram of flow between mutually opposed jets.

singular flows containing rotational components. In general the velocity gradient tensor for a two dimensional flow with a rotation component will have the form

$$\dot{\epsilon}_{ij} = \begin{bmatrix} \dot{\epsilon}_{11} & \dot{\epsilon}_{12} & 0 \\ \dot{\epsilon}_{21} & \dot{\epsilon}_{22} & 0 \\ 0 & 0 & 0 \end{bmatrix} \tag{14}$$

Following Frank [11] it is instructive to consider the 2D singular flow which is governed by the stream potential,

$$\phi = \tfrac{1}{2}\omega(x^2 + y^2) + \tfrac{1}{2}S(x^2 - y^2) \tag{15}$$

The streamlines of the flow can have distinct forms depending on the relative magnitude of ω and S. The spectrum of flows that can be obtained are shown in Fig. 7. Both the contours of the streamlines and the forms of the associated stream potential surfaces are shown. When $\omega = 0$ the flow is that of pure shearing flow and the asymptotes of the hyperbolic critical point intersect orthogonally. When $S > \omega$ the flow still contains a hyperbolic critical point, however the asymptotes no longer cut orthogonally. When $\omega = S$ a degenerate flow occurs which corresponds to the much studied simple shearing flow. When $S < \omega$ a closed orbit flow occurs where the singularity is defined by an elliptical critical point. This spectrum of flows has been explored experimentally for Newtonian fluids by Giesekus [4] using a modified four roll mill apparatus. In this experiment the drives of diagonally opposite pairs of rollers are driven independently and at variable speeds. To obtain elliptic critical points the sense of rotation of each pair of rollers must be the same, whereas to generate hyperbolic critical points adjacent rollers generally rotate in the opposite sense.

It was found by Frank and Mackley [1] that by using two co-rotating rollers flows where $S > \omega$ could be explored. The general flow for two co-rotating rollers is shown in Fig. 8. The form of the streamlines near the hyperbolic critical point at the centre of the flow obey the stream potential given by eqn. (15) and the asymptotic angle α, defined as the obtuse angle between the asymptotes, is given by

$$\cos 2\alpha = -\omega/S \tag{16}$$

This angle α is a direct measure of the relative magnitude of ω and S and can be changed by varying the separation of the rollers, consequently flows with different components of ω/S can be achieved ranging in principle from $\omega = S$ when the rollers are touching and $\omega \to 0$ when the rollers are a great distance apart.

We now consider a flow which under rather special conditions possesses a critical point which has three inflows and three outflows. This flow is represented by the stream function,

$$\phi = \gamma(\tfrac{1}{3}x^3 - xy^2) \tag{17}$$

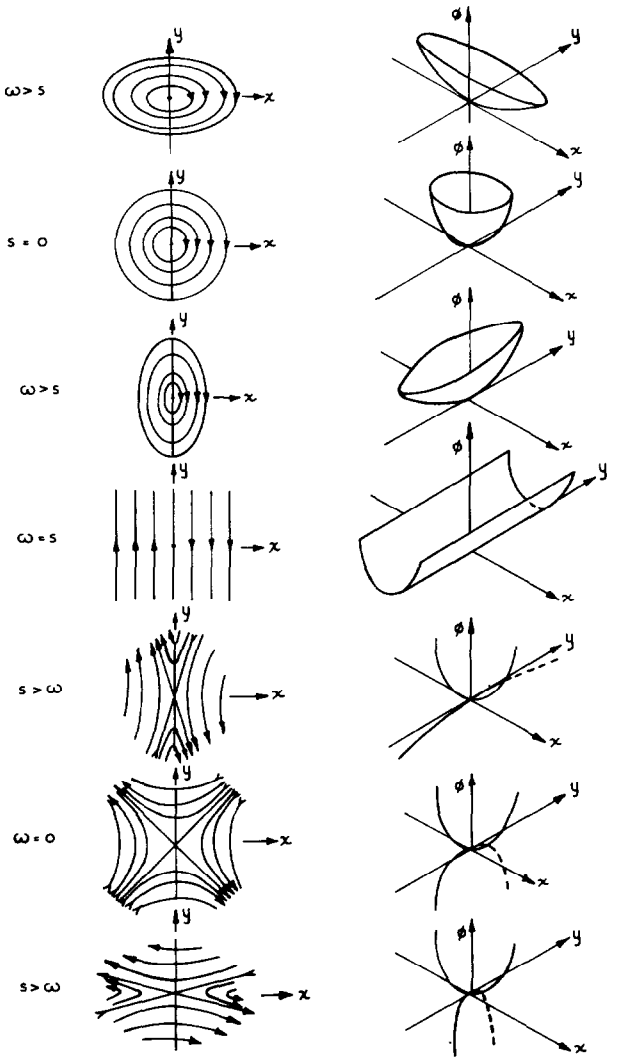

Fig. 7. Sequence of streamlines and corresponding potential surfaces for flows given by $\phi = \frac{1}{2}\omega(x^2 + y^2) + \frac{1}{2}S(x^2 + y^2)$.

The form of the flow's streamlines is shown in Fig. 11 flow number 1, and was first examined by Berry and Mackley [12]. The flow can be generated to a very good approximation by an array of six rollers symmetrically positioned, which are rotating with equal speeds in directions indicated in Fig. 9. This symmetric flow is special in that it represents a highly degenerate situation. The critical point defined as the elliptic umbilic critical point occurs at the centre of the flow and satisfies the conditions $V = 0$, $\omega = S = 0$.

The symmetry of this flow can be broken in a number of ways. Using the

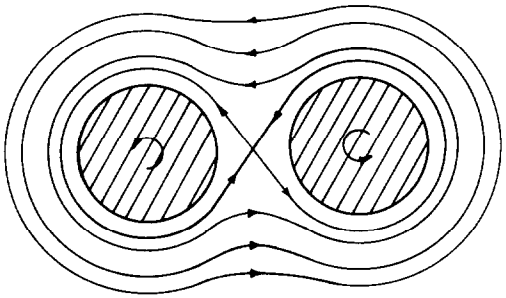

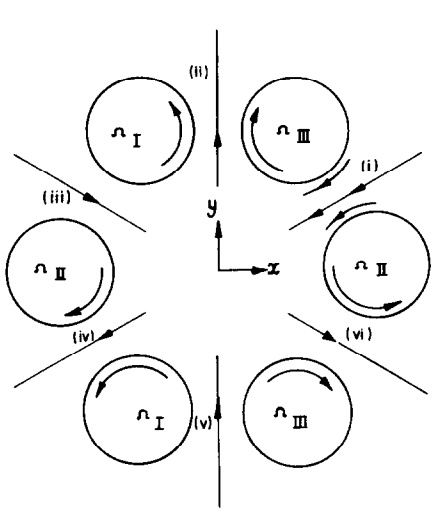

Fig. 8. Schematic diagram of flow between co-rotating rollers.

Fig. 9. Six roll mill geometry.

classification of Thom [13], Berry and Mackley [12] were able to show that only three perturbation parameters were necessary to explore all possible flows originating from the "germ" of the flow given by eqn. (17). These parameters consisted of additional translational components V_x and V_y and an additional rotational component ω. When these components are included the stream potential takes the form

$$\phi = \gamma(\tfrac{1}{3}x^3 - xy^2) - \tfrac{1}{2}\omega(x^2 + y^2) - V_y x + V_x y \tag{18}$$

These additional terms can be experimentally introduced by varying certain roller rotation rates. For example with the roller coupling shown in Fig. 9 an increase or decrease of Ω_{II} with respect to Ω_I and Ω_{III} would introduce a V_y component to the flow. Similarly an increase or decrease of Ω_{III} with respect to Ω_I would introduce a rotational component ω into the flow.

Starting from the most degenerate case, $\omega = S = 0$, additional terms in V_x, V_y and ω can be added to the flow. This has the effect of immediately changing the form that the critical points take. In order to follow how the form of critical points will change it is very useful to consider the so called "catastrophe surface" [12] of the elliptic umbilic which is shown in Fig. 10. This surface drawn in the three dimensional control space with V_x, V_y and ω as orthogonal axes, corresponds to the surface in control space where the condition $\omega = S$ is satisfied. When the parameters V_x, V_y, ω are such that the point in control space does not lie on the catastrophe surface, then $\omega \neq S$ and the critical points where $V = 0$ will either be elliptic critical points or hyperbolic critical points. When the point in control space does lie on the catastrophe surface, then $\omega = S$ and a degenerate situation occurs where a

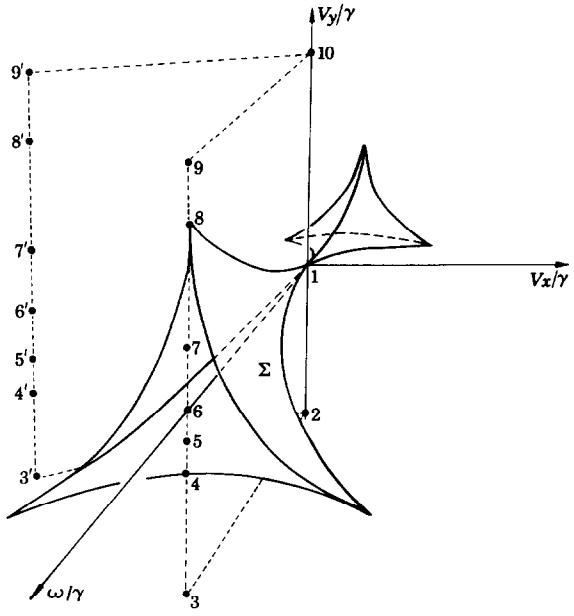

Fig. 10. Elliptic umbilic catastrophe surface in control space (from ref. [12]).

degenerate critical point associated with points $V = 0$, $\omega = S$ will exist. The forms that the degenerate critical points can take are limited and all are revealed if the path 1—10, shown in Fig. 10 is taken in control space. Fig. 11 shows the streamlines corresponding to each position 1—10 in control space.

The critical points existing at each marked position 1—10 are listed below; when the catastrophe surface is cut the number and nature of the critical points change.

Position in Fig. 10	Number and form of critical points
1	one elliptic umbilic critical point
2 and 3	two hyperbolic critical points
4	two hyperbolic critical points and one fold catastrophe critical point
5, 6 and 7	three hyperbolic critical points and one elliptic critical point
8	one hyperbolic critical point and one cusp catastrophe critical point
9 and 10	two hyperbolic critical points

The extension of the work to singularities in three dimensional flows where rotational components are present has not been made. The non degenerate three dimensional singular flows of relevance to fluid mechanics are the col which is rotation free and experimentally well represented by the opposed jet system. The three dimensional singular point containing rotational components is the col-foyer shown schematically by Fig. 12. This flow

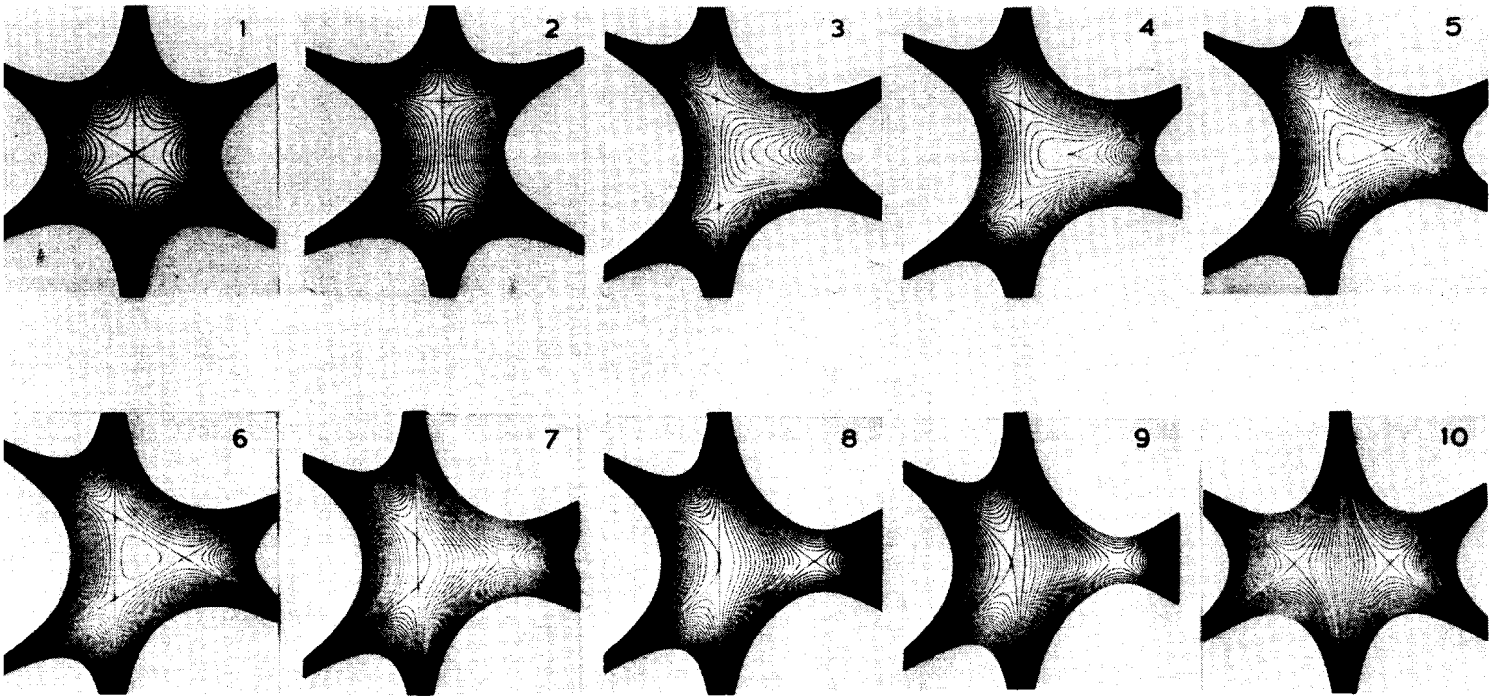

Fig. 11. Computer simulations of flows corresponding to positions 1—10 shown in Fig. 10 (from ref. [12]).

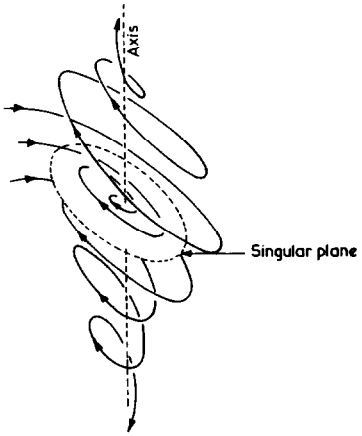

Fig. 12. The col foyer singularity (from ref. [10]).

could conceivably be generated experimentally using opposed jets with an additional device such as an offset inlet for providing circulation of the flow.

3. Flow singularities and chain extension

3.1 Theoretical considerations

Early studies of the flow behaviour of dilute polymer solutions were limited to simple shearing flows, see for example reviews by Cerf [14]. Ziabicki [15] was the first to consider theoretically rotation free flows; this study was followed by amongst others work from Peterlin [16], Frank [17] and Hlavacek and Seyer [18], Marruci [19], Hinch [20] and DeGennes [21]. Concerning rotation free flows, the essential point to emerge initially from these studies was that significant chain extension could in principle be achieved provided a certain minimum velocity gradient S was exceeded.

In terms of chain stretching the molecular parameter of importance is the relaxation time τ of the molecule. This relaxation time is a measure of the time the molecule would take to return to its random configuration if initially deformed and then allowed to relax by thermal motion. The relaxation time is dependent on the molecular weight of the chain, increasing with increasing molecular weight with typical values of τ ranging from 10^{-6}—1s (see, for example, ref. [9]).

When a polymer chain is subjected to rotation free velocity gradients there are essentially two competing forces operating. The velocity gradient is attempting to stretch the normally random chain due to fluid streaming around the chain. Opposing this stretching motion there is the "elastic entropy" force attempting to restore the chain to its preferred random configuration. All the current theories for the dilute solution behaviour of poly-

mer chains in uniform rotation free velocity gradients show a characteristic feature in that to obtain high chain extension the condition,

$$S\tau \geqslant 1, \qquad \text{(rotation free flow)} \tag{19}$$

must be satisfied. If $S\tau < 1$ the chain can to a first approximation be considered essentially undeformed with the entropic restoring forces dominating. If $S\tau \geqslant 1$ the chain can be considered to be fully extended with the hydrodynamic stretching forces dominating over the elastic retraction. As the polymer chain becomes stretched the ends of the molecule find themselves in regions of increasingly different velocities; this has the effect of significantly increasing the interaction between the chain and the flow which causes the so-called extensional viscosity to increase. Theory predicts [16] that with full chain extension increases in extensional viscosity of about one thousand can be expected.

A second necessary condition to stretch chains concerns the time required to stretch the chain. For full chain extension the ends of the chain must be stretched from their normal root mean square end-to-end distance given for a random coil by $l_0 = a\sqrt{n}$, where n is the number of repeat units and a the length of each repeat unit. The fully stretched chain has an end-to-end length $l_E = na$; thus the strain required to stretch the chain is $e = l_E/l_0$ and for a typical polymer would be of magnitude 10^2—10^3. In order to stretch the chain the chain must be in the stretching field for sufficient time to be extended by this amount. This condition can approximately be expressed by

$$St >> 1, \qquad \text{(rotation free flow)} \tag{20}$$

where t is the time the chain has been subjected to the uniform velocity gradient S.

The addition of rotational components to the flow has not been rigorously introduced into the theoretical studies on chain extension except for the special case of simple shearing flow (see, for example, ref. [16]). The calculations on simple shearing where $\omega = S$ showed that for flexible chains the degree of chain extension achieved was very small even for high velocity gradients, the reason being for this flow the rotational components of the flow become important and the molecules rotate rather than become stretched in any one direction for a sufficient period of time to become aligned.

Frank and Mackley [1] argue that rotation can be introduced by the replacement of the principal strain rate by another parameter, the persistent strain rate σ. This can most easily be shown for the two dimensional flow produced by co-rotating rollers and shown in Fig. 13. Polymer chains entering the central region of the flow near the hyperbolic critical point will align parallel to the exit asymptote of the flow and will be stretched in a direction along this asymptote. The magnitude of the strain rate that the molecule will persistently experience will be the magnitude of the strain rate along this asymptote and not the magnitude of the principal strain rate which in fact acts along lines at 45° to the ordinate axis. The persistent strain rate σ can be

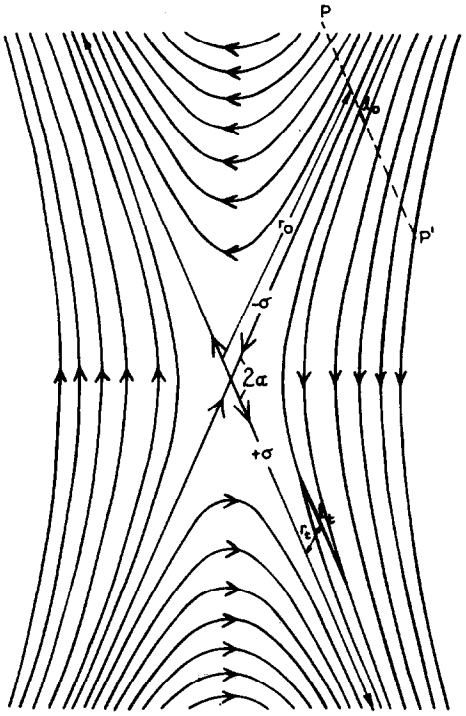

Fig. 13. Schematic diagram showing the deformation of a fluid element of initial length l_0 in a hyperbolic critical point flow.

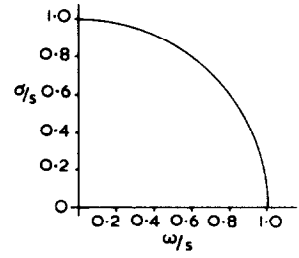

Fig. 14. Graph of persistent strain rate σ as a function of rotation rate ω.

written in terms of S and ω by,

$$\sigma = \sqrt{S^2 - \omega^2} \tag{21}$$

Thus the conditions for high chain extension given by eqns. (19) and (20) for rotation free flows may now be written in terms of the persistent strain rate giving

$$\sigma\tau \geqslant 1 \tag{22}$$

$$\sigma t >> 1. \tag{23}$$

The magnitude of the persistent strain rate as a function of ω is plotted in Fig. 14. For pure shearing flow $\omega = 0$ and $\sigma = S$; σ has its maximum value and consequently rotation free flows are the most efficient chain extenders. For simple shearing flows $\omega = S$, $\sigma = 0$; thus neither of the conditions given by eqns. (22) and (23) can be satisfied and high chain extension is not possible. Simple shearing flow marks a transition point where if $S > \omega$, σ is positive and real and if $\omega > S$, σ is imaginary. This latter case corresponds to an

oscillatory solution where rotation dominates preventing any possibility of high chain extension. The form of the curve shown in Fig. 14 shows that a certain degree of rotation component ω can be introduced into the flow without seriously impairing the flow's chain extending ability, for example a flow where $\omega = S/2$ has a persistent strain rate of 0.87 S compared to S for the rotation free flow.

3.2 Experimental consequences

The condition for high chain extension summarized by eqns. (22) and (23) places considerable restrictions on the ability and extent of regions of flow where polymer chains can be highly extended.

The first condition $\sigma\tau > 1$ requires that the magnitude of the persistent strain rate is sufficiently large. If the polymer chains were all of the same length and characterized by a single relaxation time τ a sharp transition in chain extension would be observed with increasing σ. The chains would become rapidly stretched at $\sigma\tau = 1$. Most polymers are however not highly fractionated and usually any one sample contains a large range of molecular weights. This means chains have a large range of τ with the highest molecular weight chains having the greatest value of τ. In addition if entanglements of polymer chains are present the spectrum of τ values can be expected to be further extended. With a broad range of τ the situation with increasing σ is less dramatic. At low σ, highly entangled and/or long molecules with large τ may satisfy the condition $\sigma\tau \geqslant 1$ and a small fraction of the molecules may be highly stretched with the other molecules remaining essentially undeformed. With increasing magnitude of σ a greater proportion of molecules will become progressively extended until all molecules will be stretched if the condition $\sigma\tau_{\min} \geqslant 1$ is reached.

The second necessary condition to achieve high chain extension $\sigma t >> 1$ may have the significant effect of localizing the regions of flow where high chain extension can be achieved [5]. The effect is directly related to the existence of a singularity in the flow where $V = 0$. The principle of localized chain extension is again well illustrated with reference to the hyperbolic critical point observed between two co-rotating rollers, shown in Fig. 13. Persistent strain rates of $+\sigma$ operate along the outgoing asymptotes of the flow and $-\sigma$ along the ingoing asymptotes. The magnitudes of the strain rates near the critical point are approximately uniform, thus the velocity along each asymptote may be written as,

$$\partial r_1/\partial t = \sigma r_1 \qquad \text{(outgoing asymptote)} \tag{24}$$

$$\partial r_2/\partial t = -\sigma r_2 \qquad \text{(ingoing asymptote)} \tag{25}$$

Assume fluid elements along a line marked PP′ in Fig. 13 are undeformed until they reach PP′ which is a distance r_0 from the origin measured parallel to the ingoing asymptote. The subsequent strain in the direction of σ of a fluid

element of initial length l_0 that enters the flow along PP' will be

$$\epsilon = l_t/l_0 = e^{\sigma t}. \tag{26}$$

At time t the element will be parallel to the outgoing asymptote and a distance r_t from the exit asymptote measured parallel to the ingoing asymptote, where r_t is given by,

$$r_t = r_0\, e^{-\sigma t} \tag{27}$$

For high chain extension $\sigma t >> 1$ thus from eqn. (26) $r_t/r_0 << 1$, consequently high chain extension can only be achieved very close to the outgoing symmetry plane of the flow. This observation is completely consistent with experimental observations with all the singular flows studied where highly localized flow birefringence corresponding to localized chain extension has been seen [1,5,9]. The degree of localization is quite striking and reflects the high strains required to stretch flexible chains.

In the case of co-rotating rollers the localized chain extension occurs as a sheet of oriented molecules along the outgoing symmetry sheet of the flow [1]. For other flows the localization always occurs along asymptotic lines, planes or sheets originating from stagnation points or lines. The position of the observed localized birefringence for certain flows is shown schematically in Fig. 15. One example of localized chain extension is also shown in Fig. 16

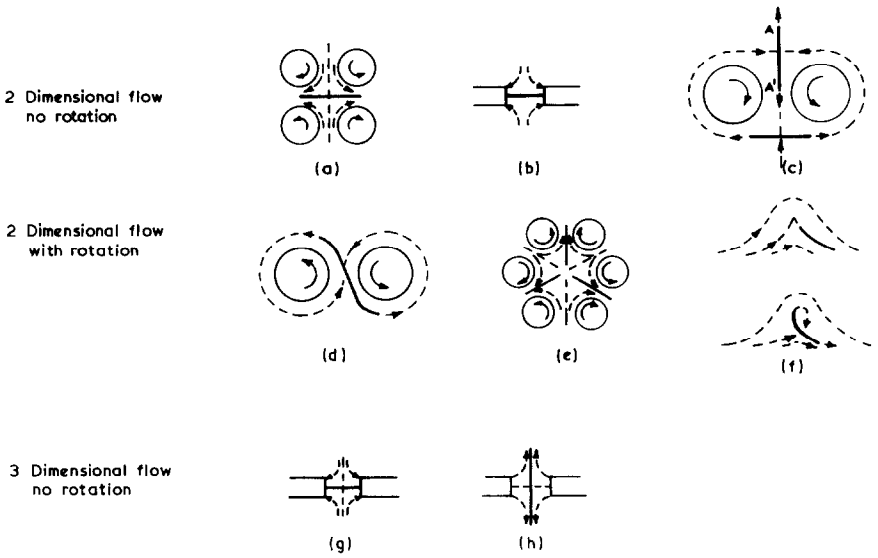

Fig. 15. Schematic diagram showing regions marked as bold lines where localized birefringence occurs for certain flows: (a) four roll mill, (b) double slit, (c) counter rotating rollers, (d) co-rotating rollers, (e) six roll mill, (f) fold catastrophe critical point and flow containing one hyperbolic critical point and one elliptic critical point, (g) axial extension (double jet), (h) axial compression (double jet).

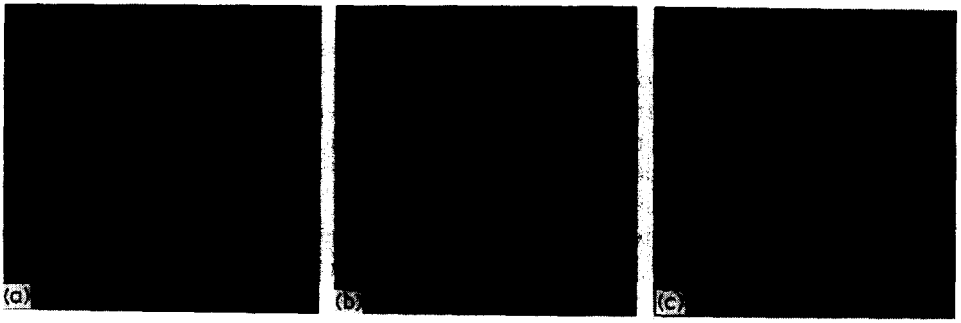

Fig. 16. Flow birefringence photographs observed between double slit apparatus viewed between diagonally crossed polaroids. Internal dimensions of slits = 1 mm × 5 cm. Photographs (a) corresponding to 0.5% polyethylene oxide (WSR 301)/water solution subject to strain rate $S \approx 320\ s^{-1}$, jet separation = 3.6 mm. (b) and (c) 1.0% polyethylene oxide (WSR 301)/water solution subject to strain rates given by (b) $S \approx 15\ s^{-1}$, (c) $S \approx 65\ s^{-1}$, jet separation = 3.0 mm. Exposure times of each photograph typically 5 sec.

from the localized flow birefringence observed for the pure shearing flow produced between double slits.

It is very difficult to visualize flow systems other than those containing singular flows where flexible polymer chains can be significantly stretched, thus singularities and high polymer chain extension become intimately related.

4. Flow singularities and hydrodynamic instability

4.1 Degenerate and non-degenerate flows

During the course of studying the flows that have been discussed in the previous sections it was found that certain flows were stable and insensitive to various perturbations whilst other flows were highly sensitive and unstable. In particular it was observed that the topological behaviour of the critical points of the flows were very sensitive markers as to whether a particular flow was stable or not.

Concerning two dimensional flows stability can most usefully be discussed in terms of the magnitude of the rotation ω of the flow and the principal strain rate S. Flows that were free from any rotation components such as the four roll mill and the double slit were found to be remarkably stable to fluctuations in roller speed and/or the introduction of polymer into the flow. Stability is indicated in the observed unchanged topology of the hyperbolic critical point where the asymptotes of the flow intersect orthogonally at the origin. To a certain extent the symmetry of the four roll mill and double slit apparatus dictates that the flow should maintain its symmetry, however another essentially rotation free flow is the flow between counter rotating rollers, shown schematically in Fig. 4, and again it was observed that the

overall topological form of the ingoing and outgoing hyperbolic critical points remained the same for perturbations such as slight mismatch of roller speeds and the addition of polymer.

A similar degree of stability was observed between co-rotating rollers where $S > \omega > 0$. The asymptotes at the hyperbolic critical point no longer cross orthogonally but the topological form of the flow remained unchanged when slight perturbations were applied [1].

The situations of greatest interest are the cases when degenerate critical points exist where $V = 0$, $\omega = S$. This occurs in the family of flows shown previously in Fig. 7. When $S > \omega$ the flow contains a hyperbolic critical point, when $\omega > S$ the flow contains an elliptic critical point. The condition $\omega = S$ marks the transition between these two situations and corresponds to simple shearing flow. If a simple shearing flow of the form shown in Fig. 7 is perturbed by, say, the addition of transverse velocity components V_x, V_y and/or ω, the flow can change into different topological forms. For example an addition of ω would change the topological form to an elliptic critical point, alternatively a decrease in ω would result in a hyperbolic critical point. Simple shearing flow therefore represents a highly unstable flow which depending on the nature of the perturbation can modify the flow into a number of different topological forms. The degeneracy and change in topology of the flow is reflected by the change in the form of the potential surfaces of the associated flows which are also shown in Fig. 7, here the potential surface changes from a surface containing a saddle point to a semitubular form at $\omega = S$ and then to a bowl like surface containing a minimum at the origin.

The transition behaviour of simple shearing flows is further enhanced by the fact that the persistent strain is real and positive when $S > \omega$ and becomes imaginary when $S < \omega$. This means that physically the behaviour for example of polymer chains, oil droplets and the formation of meterological weather fronts [22] will all be significantly different on either side of the transition point.

The above observations concerning the instability of simple shearing flow may appear surprising in that most laboratory experiments on laminar flow are carried out under simple shearing conditions and in general these flows are found to be rather stable. However if we have a simple shearing flow, in order that a perturbation can change the topology it is necessary that the degenerate critical point does not occur at a solid boundary of the flow. For example in a Couette apparatus which approximates well to simple shearing flow if the cylinders are sufficiently close to each other, the condition $V = 0$ is only satisfied on the walls of one of the cylinders, consequently whilst the stagnation sheet resides on the wall of the cylinder it is not possible for the flow to change topology in the same way as if the stagnation point was unbounded.

The significance of degenerate critical points and flow stability is very clearly shown in the six roll mill experiment [12]. If the condition $V = 0$,

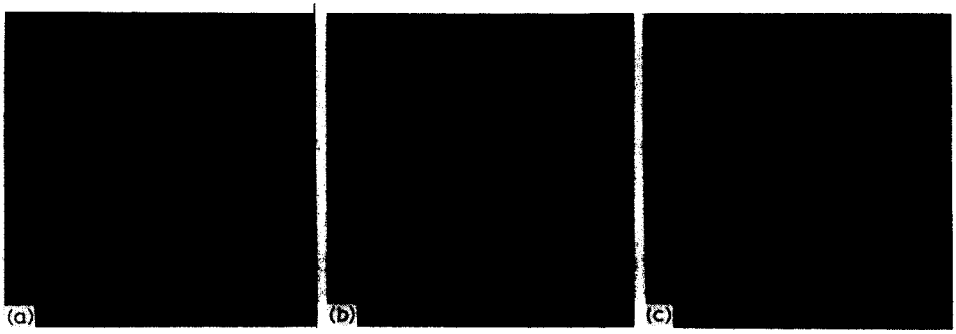

Fig. 17. Streamline photographs of six roll mill flow showing (a) one elliptic umbilic critical point, (b) two hyperbolic critical points produced by an additional $-V_y$ flow component, (c) two hyperbolic critical points produced by a further additional $-V_y$ flow component.

$\omega = S$ is satisfied a perturbation in the form of an additional V_x, V_y or ω will produce a change in the topological form of the flow. Thus flows corresponding to control settings where the elliptic umbilic catastrophe surface shown in Fig. 10 is cut are intrinsically unstable, control settings where the perturbation is insufficient to cause a cutting of the catastrophe surface are intrinsically stable and the topology will remain unchanged. By way of example, the flow corresponding to $V_x = V_y = \omega = 0$ is shown in Fig. 17a. The slightest perturbation in the form of a V_y component will break the symmetry of the flow and two hyperbolic critical points will develop, as shown in Fig. 17b. A further perturbation in terms of an additional V_y component will not produce another change in topology, the position of the hyperbolic critical points will merely move further away from the origin with increasing V_y, as shown in Fig. 17c.

A topology change of particular interest is that associated with the development of the central eddy shown by flows (3, 4, and 5) in Fig. 11. In this sequence a region of flow initially without a critical point develops and hyperbolic and elliptic critical point. The sequence is shown in Fig. 18. The initially smooth contours develop a degenerate fold catastrophe critical point which subsequently forms a hyperbolic and elliptic critical point. This sequence of flows could conceivably correspond to the development of instabilities and eddies near the boundary of a wall for an initially two dimensional laminar boundary layer flow. Consequently the sequence of flows could be related to the onset of turbulent boundary layers and could also illustrate one of many mechanisms for generating eddies which can maintain

Fig. 18. Schematic diagram showing the development of a fold catastrophe critical point.

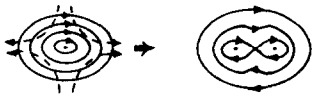

Fig. 19. Schematic diagram showing a possible mechanism for the multiplication of critical points (from Gibson, ref. [23]).

the turbulence. The intermediate turbulent situations of following the decay of large eddies to smaller eddies offers many interesting topological possibilities. In a different context a possible topological sequence is considered by Gibson [23] and is shown schematically in Fig. 19; here an elliptic critical point is deformed by an external stretching field and breaks up to form two elliptic critical points and one hyperbolic critical point.

It can be seen from these few examples that topology changes in flows such as the formation and multiplication of eddies in turbulent flows is associated with the existence of degenerate critical points in the flows.

4.2 Flow modification and instabilities due to polymer chain extension

The question of how chain extension can modify a certain flow is not easily answered; it would appear that effects become more subtle and complex with the increasing complexity of the flow being studied.

At this point it should be noted that all experiments to be described were carried out with relatively concentrated polymer solutions typically 1.0—2.0% polyethylene oxide/water. This was done for two reasons, firstly these solutions gave sufficiently high viscosities to ensure that the onset of turbulence did not occur at the range of speeds used and secondly the high polymer concentration enabled flow birefringence studies to be easily made. Recent experiments using dilute polymer solutions for double jet and slit systems have been carried out by Pope and Keller [24].

It has been stated previously that the topology and form of the rotation free flow patterns produced by the four roll mill and double slit are unchanged with the introduction of polymer even when localized high chain extension can be observed using flow birefringence techniques. Velocity measurements have not yet been made on these flows to establish whether or not the magnitude of the velocity field is reduced due to the anticipated increase in extensional viscosity.

Modifications to the flow were observed for both counter and co-rotating roller experiments. The situation for counter rotating rollers is shown clearly in Figs. 20 and 21. Glycerol behaves essentially as expected. With increasing roller separation the hyperbolic critical points move outward as shown in Fig. 20 and as predicted by Jeffreys [6]. The position of these critical points remains unchanged with increasing roller rotation as recorded in Table 1. The behaviour with an 0.8% polyethylene oxide (WSR301)/water solution is quite striking. For a given roller separation the ingoing hyperbolic critical

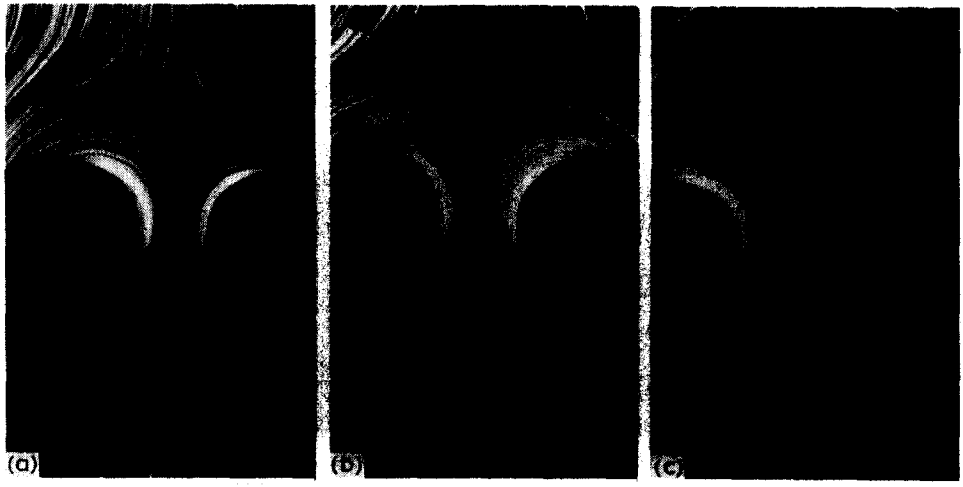

Fig. 20. Streamline photographs of flow between counter rotating rollers for a Newtonian liquid, glycerol. Diameter of rollers = 1.0 cm, flow moving vertically downwards through "throats" of rolls. Shortest distance between surfaces of each roller for each sequence, (a) = 0.56 ± 0.05 cm, (b) 0.72 cm, (c) 1.10 cm. Roller rotation rates for each sequence = 0.7 revs/sec. Exposure time 3 seconds, small quantity of Hostalen GUR powder added to glycerol to detect streamlines.

point moves outwards with increasing roller speed whilst the position of the lower stagnation point remains unchanged, as shown in Fig. 21. This feature was first recorded in 1975 and subsequently brought to the author's attention by further experiments carried out by C.J. Farrell at Bristol University.

TABLE 1

Table of distance between stagnation points as a function of roller separation and roller rotation rate for counter rotating rollers. Roller diameter = 1 cm

Fluid	Roller rotation rate (rev/sec)	Roller separation, minimum distance between surfaces of rollers (cm)	Distance between stagnation points (cm)
glycerol	0.7	0.56	2.19 ± 0.08
	0.7	0.72	2.53 ± 0.08
	0.7	1.10	4.09 ± 0.08
glycerol	0.3	0.72	2.63 ± 0.08
	0.7	0.72	2.53 ± 0.08
	1.0	0.72	2.63 ± 0.08
	1.4	0.72	2.59 ± 0.08
0.8% polyethylene oxide (WSR 301)/ water	0.3	0.47	2.3 ± 0.08
	0.7	0.47	2.43 ± 0.08
	2.1	0.47	2.69 ± 0.08

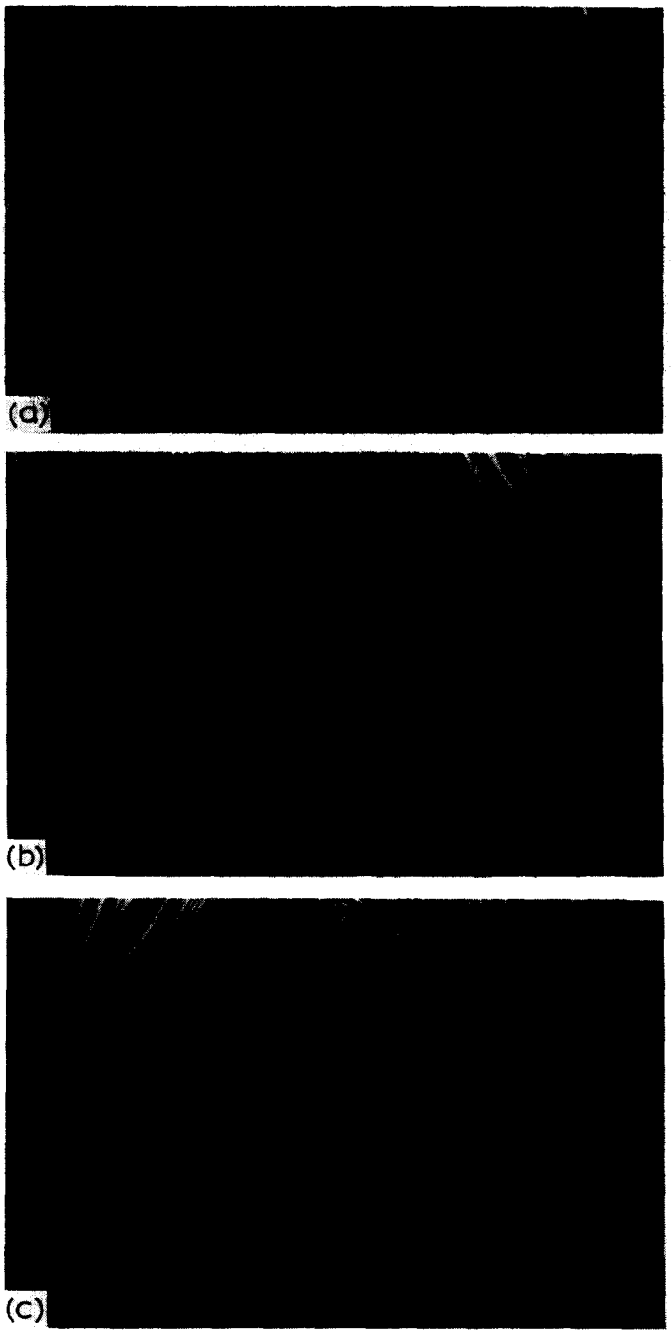

Fig. 21. Streamline photographs of flow between counter rotating rollers for a 0.8% polyethylene oxide (WSR 301)/water solution. Diameter of rollers = 1.0 cm, flow moving vertically downwards through "throats" of rolls. Shortest distance between surfaces of each roller = 0.47 ± 0.02 cm. Roller rotation rates for each sequence (a) 0.3 revs/sec, (b) 0.7

The outward movement of the ingoing stagnation point can be qualitatively explained by polymer chains becoming locally stretched with increasing rotation rate in the region marked AA′ in Fig. 15 close to the exit symmetry plane of the hyperbolic critical point; this would have the effect of increasing the extensional viscosity in this region. In order to reduce the subsequent enhanced stress levels in the fluid the magnitude of the locally applied persistent strain rate is correspondingly reduced by the outward movement of the ingoing hyperbolic critical point. Thus chain extension in this rotation free flow appears to result in a modification of the flow which attempts to reduce the σ component of the flow when the molecules are being stretched. The justification for anticipating localized molecular extension in the region AA′ in Fig. 15c is supported from the localized flow birefringence observations in the four roll mill [5] and double slit systems where the flows are essentially identical in the region of the hyperbolic critical point. In addition, recent observations in Bristol [25] and Strasbourg [26] have confirmed the existence of localised flow birefringence in the counter-rotating two roll mill.

The flow modification produced by the presence of polymer for the case of co-rotating rollers has been previously reported by Frank and Mackley [1]. For a roller separation giving a hyperbolic cricial point with non orthogonal asymptotes where $\omega/S = 0.53$ and $\sigma = 0.845$ it was found that for a glycerol solution the asymptote angle α defined by eqn. (16) remained constant with increasing roller speed. The situation when a 1.0% polyox, WSR301/water solution was introduced was different, here the asymptotic initially at a value of $\alpha = 129°$ increased with increasing roller rotation rate to a value of $\alpha = 145°$. Using eqn. (16) this change in angle can be associated with an increase in ω/S, thus either the principal strain rate decreases or the rotation rate increases or both. From eqn. (21) it can be seen that an increase in ω/S must correspond to a decrease in the persistent strain rate σ. Because the experimental conditions are such that the values of S and ω are significantly different even with the addition of polymer no change in topology of the flow was expected or observed. In the co-rotating roller situation where a rotational component of the flow is present it appears that the effect of localized chain extension along the exit symmetry sheet of the flow has the effect of reducing the magnitude of the persistent strain rate.

The flow modification produced by the presence of polymer in the six roll mill was reported by Berry and Mackley [12]. The observed effect was quite subtle and serves to illustrate the complexity of possible flow modifications. Many of the flows explored using the six roll mill which are schematically shown in Fig. 11 occur near or on the catastrophe surface shown in Fig. 10, this means that for these flows the conditions $\omega = S$ is nearly satisfied. In this situation the modification of the flow due to the presence of polymer is sufficient in some circumstances to result in a transition across the $\omega = S$ catastrophe surface with the result that a change in the topology of the flow is possible.

When polymer was introduced into the systems and roller settings chosen to take a path 1—10 in control space shown in Fig. 10, it was found that the topology of the observed flows in fact corresponded to a path 1, 2, 3′ ... 9′, 10 also shown on Fig. 10 where in particular flows contained two hyperbolic critical points and no eddy was generated [12]. These observations require that the catastrophe surface is not cut except at the origin. To achieve this an additional V_x component to the flow has to be accounted for. With the roller couplings of the form used it is initially difficult to visualize how this can happen, however flow birefringence observations help in interpreting behaviour. For all the flows examined chain extension if it occurs at all will be seen localized on the outgoing asymptotes of the flow which eventually pass through the throats of the roller gaps (ii), (iv) and (vi) marked in Fig. 9. If a localized enhanced viscosity caused by the local chain extension is associated with the outgoing flows (ii), (iv) and (vi), this can have the effect of breaking the symmetry of the out- and ingoing flow profiles between the throats of the rollers. The effect of this is quite subtle, if there is no rotation present, $\omega = 0$, flow profiles through throats marked (i), (iii), (iv) and (vi) in Fig. 9 are all the same and the symmetry breaking of inflow and outflow velocity profile is still insufficient to produce an overall V_x component in the central region of the flow and the flow remains unchanged. If there is a rotational component to the flow, flows marked (i) and (vi) have different values of velocity profiles to (iii) and (iv) and in this case symmetry breaking results in different inflow and outflow velocity profiles and can produce an additional V_x component. It was thus found that rotation free flows were unchanged with the addition of polymer but the topology of all flows containing rotation was changed when the polymer was added. Both observations are consistent with localized enhanced viscosities reducing the persistent strain rate in these regions and thereby modifying the velocity profile in specific regions of the flow.

To summarize, the observations of this section, it has been observed that singular flows containing hyperbolic critical points with $\omega = 0$ do not change topology or develop rotational components with the addition of polymer, however the position of the hyperbolic critical point can be significantly displaced in an apparent attempt to reduce the local persistent strain rate in the region where molecules are being stretched. Similarly flows where $S > \omega > 0$ are modified by the presence of polymer in a way that the persistent strain rate σ decreases. Finally flows that occur near degenerate critical points where $\omega = S$ could be subjected to a change in topology and a local reduction in a persistent strain rate in the region of the outgoing asymptotes emerging from the critical or degenerate critical point in question.

5. Conclusion

The overall observations of the experimental work reviewed in this paper strongly suggest that the behaviour of critical points in steady flow is of im-

portance in terms of understanding factors associated with high chain extension of polymers and also general problems related flow modification and instability. The achievement of high chain extension has many practical applications mainly resulting from the large anisotropic properties which develop when the chains are stretched. The way polymers modify flows is of importance to plastics processing and also to the increasing practice of using polymers as additives to modify rheological properties of fluids.

From the experimental observations presented in this paper the subtle way polymers can modify relatively simple flows suggests that generalizations are difficult to make with confidence; however at this stage all experimental observations reported here have shown plausible agreement with the concept that the addition of polymer to a flow causes a reduction in the magnitude of the persistent strain rate in the region of flow where polymer chains have been appreciably stretched.

Finally, the study of the behaviour of critical points in complex fluid flow situations appears to be a powerful way of both characterizing the flow as well as obtaining physical information concerning the development and interactions of the flow.

Acknowledgements

The experimental work described in this paper was carried out at the H.H. Wills Physics Laboratory, Bristol. The invaluable contributions of Sir Charles Frank, Professor A. Keller and Dr. M.V. Berry to the work are acknowledged. Miss R. Blackburn and Mr. D. Duhig are also to be thanked for carrying out the preliminary studies using the double slit system.

References

1 F.C. Frank and M.R. Mackley, J. Polymer Sci., A2, 14 (1976) 1121.
2 F.T. Trouton, Proc. Roy. Soc. London, A77 (1906) 426.
3 G.I. Taylor, Proc. Roy. Soc. London, A146 (1934) 501.
4 H. Giesekus, Rheol. Acta, 2 (1962) 112.
5 D.G. Crowley, F.C. Frank, M.R. Mackley and R.G. Stephenson, J. Polymer Sci., A2, 14 (1976) 1111.
6 G.B. Jeffrey, Proc. Roy. Soc. London, A101 (1922) 169.
7 H. Werlé, Ann. Rev. Fluid Mech., 5 (1973) 361.
8 F.C. Frank, A. Keller and M.R. Mackley, Polymer, 12 (1971) 467.
9 M.R. Mackley and A. Keller, Phil. Trans. Roy. Soc. London, A278 (1975) 29.
10 F.R.N. Nabarro, J. Physique, 33 (1972) 1089.
11 F.C. Frank, Invited lecture at 50th Anniversary of the Canadian Pulp and Paper Institute, Montreal, 1975.
12 M.V. Berry and M.R. Mackley, Phil. Trans. Roy. Soc. London, A287 (1977) 1.
13 R. Thom, Stabilité structurelle et morphogénèse, Reading, Mass., Benjamin 1972 (English translation 1975).
14 R.C. Cerf and H.A. Scherega, Chem. Rev., 51 (1952) 185.
15 A. Ziabicki, J. Appl. Pol. Sci., 2 (1959) 14.
16 A. Peterlin, Pure Appl. Chem., 12 (1966) 563.

17 F.C. Frank, Proc. Roy. Soc. London, A319 (1970) 127.
18 B. Hlavacek and F.A. Seyer, Kolloid Z. Z. Polymere, 243 (1971) 32.
19 G. Marruci, Polymer Eng. Sci., 15 (1975) 229.
20 J. Hinch, J. Fluid Mech., 74 (1976) 317.
21 P. De Gennes, J. Chem. Phys., 60 (1974) 5030.
22 S. Petterson, Introduction to Meteorology, McGraw-Hill, 1969, p. 220.
23 C.H. Gibson, The Physics of Fluids, 11 (1968) 2305.
24 D.P. Pope and A. Keller, submitted to J. Colloid Polymer Sci.,
25 C.J. Farrell and A. Keller, private communication.
26 R. Cressely, H. Hocquart and O. Scrivener, submitted to Optica Acta.